Scattering Matrix of a Reciprocal and Lossless, Three-Port Power Divider

Antonio Morini, Tullio Rozzi, Marco Farina, *Senior Member, IEEE*, and Piero Angeletti, *Life Fellow, IEEE*

***Abstract*— The analytical expression of the scattering matrix of a lossless, reciprocal three-port junction is derived using three arbitrary real angles. This derivation extends a previously proposed method that was limited to cases with a plane of symmetry. The derived formulas are validated analytically and confirmed through both full-wave analysis of a stripline divider and experimental measurements of a strongly asymmetrical and a quasi-symmetrical waveguide divider.**

***Index Terms*— BFN, diplexer, divider, scattering matrix, slot arrays, substrate integrated waveguide, three-ports, waveguide antennas.**

I. Introduction

THREE-PORT junctions represent a fundamental building block of any microwave system, namely dividers, diplexers, BFNs, and antennas, and their properties are discussed in classical microwave textbooks [1], [2], [3], [4], as well as in older and more recent papers [5], [6], [7], [8], [9], [10], [11], [12], [13], [14].

Nevertheless, their scattering matrix is analytically known only for the special cases of branched transmission lines [5]. Only recently, the explicit formulas of the scattering matrix of a lossless reciprocal three-port junction with a plane of symmetry has been presented in the literature [15].

In this article, we extend the approach of [15] to the asymmetrical case and derive an analytical expression of the scattering matrix of an arbitrary lossless reciprocal three-port junction, in terms of three bounded real parameters. The article is organized as follows.

Formulation of the theorem: The article begins with the formulation of a theorem that establishes the general form of the scattering matrix of any reciprocal and lossless three-port junction.

Examples and validation: Next, the article presents examples of relevant cases and validations through full-wave simulations and experimental results.

Analytical Proof: Finally, the article includes an analytical proof to rigorously demonstrate the correctness of the theorem.

Received 1 February 2024; revised 29 April 2024 and 28 August 2024; accepted 7 September 2024. Date of publication 26 September 2024; date of current version 8 November 2024. *(Corresponding author: Antonio Morini.)*

Antonio Morini, Tullio Rozzi, and Marco Farina are with the Dipartimento di Ingegneria dell'Informazione, Università Politecnica delle Marche, 60131 Ancona, Italy (e-mail: a.morini@univpm.it).

Piero Angeletti is with European Space Agency, 2200 AG Noordwijk, The Netherlands (e-mail: piero.angeletti@esa.int).

Color versions of one or more figures in this letter are available at https://doi.org/10.1109/LMWT.2024.3460168.

Digital Object Identifier 10.1109/LMWT.2024.3460168

II. Expression of a Reciprocal Lossless Three-Port

It is well known that the scattering matrix of an arbitrary lossless reciprocal N-port linear device can be expressed in terms of $N \cdot (N+1)/2$ real parameters, which reduce to $N \cdot (N-1)/2$ when the reference planes are properly chosen (3 Sec 3.3 p. 120 "Transformation of Reference Planes"), namely three, for the three-ports. So, given the scattering matrix of a reciprocal loss-less three-port

$$\mathbf{S} = \begin{bmatrix} S_{11} & S_{12} & S_{13} \\ S_{12} & S_{22} & S_{23} \\ S_{13} & S_{23} & S_{33} \end{bmatrix}$$

it is expedient to set the reference planes in a way that S_{33}, S_{23}, and S_{13} are all real [3], [4].

The port numbering adopted, in which port 3 represents the input, derives from the habit of working with diplexers, indeed one of the most common applications of three-port junctions. In this case, it is quite convenient to use the same number for the filter and for the port of the junction which the filter is connected to [8].

With this choice, the following theorem holds.

The scattering matrix of any lossless and reciprocal three-port is given by:

$$S_{33} = \cos\vartheta, \quad S_{13} = \sin\vartheta\cos\tau, \quad S_{23} = \sin\vartheta\sin\tau \tag{1a}$$

$$S_{12} = -\cos\tau\sin\tau\cos\sigma\cos\vartheta\left(1 \mp \sqrt{1+\frac{\tan^2\vartheta}{\cos^2\sigma}}\right)e^{j\sigma} \tag{1b}$$

$$S_{11} = -S_{12}\tan\tau - \cos\vartheta \, S_{22} = -S_{12}/\tan\tau - \cos\vartheta \tag{1c}$$

where ϑ, τ, and σ are real parameters that, because of the periodicity of the trigonometric functions, are confined to the interval $(-\pi, \pi)$. The power division ratio (PDR) is given by $|S_{23}/S_{13}|^2 = \tan^2\tau$, the reflection magnitude at port 3 is $|\cos\vartheta| = |S_{33}|$ and $\sigma = \arg(S_{12})$. The latter influences both magnitudes and phases of S_{12}, S_{11}, and S_{22}. Once $|S_{33}|$ and PDR are set, $|S_{12}|$ depends solely on σ, according to (1b), with the sign specified in [(11a)–(11b)].

III. Special Cases

Three-port with a symmetry plane, as a T-junction with port 3 taken as input. The expressions (1a)–(1c) are equal to (1a) and (1b) of [15], provided that the following equations hold:

H-plane

$$\tau = \frac{\pi}{4}, \sigma = \pi + \tan^{-1}\frac{\sin\varphi}{\cos\varphi + \cos\vartheta} \tag{2a}$$

E-plane

$$\tau = -\frac{\pi}{4}, \sigma = \tan^{-1}\frac{\sin\varphi}{\cos\varphi + \cos\vartheta}. \tag{2b}$$

The above formulas show the consistency of the present derivation with the one obtained for the junction with a symmetry plane. As expected, in the symmetrical case, the scattering matrix only depends on two real parameters, namely φ and ϑ, where (2a) and 2(b) link the real parameter σ, used in this article, to φ, used in [10].

Note that the symmetrical Price-Leichtner *1:N* divider (PLD), with $N = 2$ [5], falls in the H-plane category. In fact, when the ports are numbered as in this article (namely, ports 1, 2, 3 of PLD, respectively, corresponds to ports 3, 1, 2 of this model), its scattering parameters are $S_{33} = 0$, $S_{11} = S_{22} = -1/2$, $S_{13} = S_{23} = 1/\sqrt{2}$, $S_{12} = 1/2$ [5]. This is a particular form of the proposed scattering matrix, where the relevant parameters are: $\vartheta = \pi/2$, $\tau = \pi/4$, $\sigma = 0$.

Actually, the renumbering of the ports, carried out for the sake of clarity, is not strictly necessary. If the original numbering of [5] were kept, the values of the relevant parameters would be: $\vartheta = 2\pi/3$, $\tau = 0.615$, $\sigma = 0$, thus proving once more the generality of the proposed model.

– Asymmetrical in-phase divider matched at the input port.

The general form of the scattering matrix of an ideal asymmetrical lossless reciprocal three-port matched at the input (port 3), as the ones forming the building blocks of a complex 1:64 reactive beam forming network measured in [17] is given by

$$\begin{bmatrix} (1-m^2)e^{j\varphi_{11}} & m\sqrt{1-m^2}e^{j\varphi_{12}} & me^{j\varphi_{13}} \\ m\sqrt{1-m^2}e^{j\varphi_{12}} & m^2e^{j\varphi_{22}} & \sqrt{1-m^2}e^{j\varphi_{23}} \\ me^{j\varphi_{13}} & \sqrt{1-m^2}e^{j\varphi_{23}} & 0 \end{bmatrix} \tag{3}$$

where because of losslessness, the phases $\varphi_{ij} = \arg(s_{ij})$ are constrained by the equations:

$$\varphi_{11} = \varphi_{12} + \varphi_{13} - \varphi_{23} \pm \pi \tag{4a}$$

$$\varphi_{22} = \varphi_{12} - \varphi_{13} + \varphi_{23} \mp \pi. \tag{4b}$$

The equi-phase case occurs when $\varphi_{23} = \varphi_{13}$. Without loss of generality, the latter may be set equal to 0. Therefore, the resulting scattering matrix is

$$\begin{bmatrix} -(1-m^2)e^{j\varphi_{12}} & m\sqrt{1-m^2}e^{j\varphi_{12}} & m \\ m\sqrt{1-m^2}e^{j\varphi_{12}} & -m^2e^{j\varphi_{12}} & \sqrt{1-m^2} \\ m & \sqrt{1-m^2} & 0 \end{bmatrix}. \tag{5}$$

It is straightforward to verify that this form can be derived by the expressions (1a)–(1c), by setting $\varphi_{12} = \sigma$, $m = \cos\tau$, and $\cos\vartheta = 0$.

IV. Verification

As a practical example, we simulated the unbalanced stripline 2-dB divider of Fig. 1 (left) [Rogers 5880 and Copper, strip widths (mm) 2.8, 2.6, and 1.025; dielectric and conductor thicknesses (mm) 3.15 and 0.35, respectively].

The reference planes are chosen in a way that S_{33}, S_{23}, and S_{13} are all real positive. The latter are combined with S_{12}, by 1c, to find out $\hat{S}_{11}$ and $\hat{S}_{22}$, which are compared with

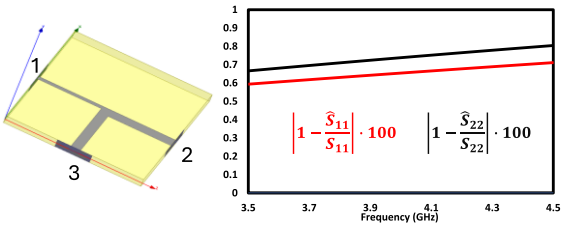

Fig. 1. Left-Sketch of the 2 dB imbalanced strip-line divider simulated by HFSS, Right-Percentage relative errors between simulated (S_{11} and S_{22}) and calculated by (1c) ($\hat{S}_{11}$ and $\hat{S}_{22}$) reflections.

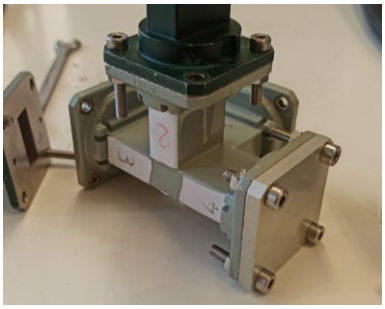

Fig. 2. Magic-T, with one port of the collinear arms shorted (port 4), to make the resulting three-port strongly asymmetrical.

the parameters S_{11} and S_{22} directly outcoming from HFSS (Fig. 1 Right).

As can be observed, the percentage relative deviations between $\hat{S}_{ii}$ and S_{ii} ($i = 1,2$) remain below 0.8%. When lossless materials are used, they decrease further, dropping to less than $60 \cdot 10^{-9}$%, with our solver settings. In order to validate experimentally the reliability of the expression (1a)–(1c) when dealing with real situations, we have measured two waveguide, nearly lossless, X-band three-port junctions, namely a commercial unmatched Magic-T, with one collinear arm shorted to make the geometry of the resulting three-port strongly asymmetrical (Fig. 2), and an X-band E-plane T-junction, available in our lab and already used in [15] which, because of some fabrication inaccuracy, exhibits a weak geometrical asymmetry. In both cases, we start from the measurement of $\bar{S}_{33}$, $\bar{S}_{31}$, and $\bar{S}_{32}$, and shift the reference planes in order to obtain real positive S_{33}, S_{31}, and S_{32}. These shifts are performed by adding—at each port and for each frequency spot—lossless line sections of lengths $l_3 = \arg(\bar{S}_{33})/(2\beta)$, $l_2 = \arg(\bar{S}_{32})/\beta - l_3$ and $l_1 = \arg(\bar{S}_{31})/\beta - l_3$ (4, p. 250).

With the new reference planes, the measured scattering matrix, $\bar{\mathbf{S}}$, is transformed into $\mathbf{S}$, by the equation (4, p. 250)

$$S_{ij} = \bar{S}_{ij}e^{-j\beta(l_i+l_j)}. \tag{6}$$

Next, from S_{33}, S_{31}, S_{32} and $\arg(S_{12})$, by (1a) and (1b), we determine the relevant parameters:

$$\vartheta = \cos^{-1}(S_{33}), \quad \tau = \tan^{-1}(S_{23}/S_{13}), \quad \sigma = \arg(S_{12}). \tag{7}$$

Once the values of the parameters (7) have been calculated, the scattering matrix $\hat{\mathbf{S}}$ is constructed using (1a)–(1c).

Note that $\hat{\mathbf{S}}$ does not represent the best approximation of the measured $\mathbf{S}$, as it would be if the triplet ϑ, τ, and σ, had been chosen as best approximated solution of the overdetermined system of the six (1a)–(1c) [16].

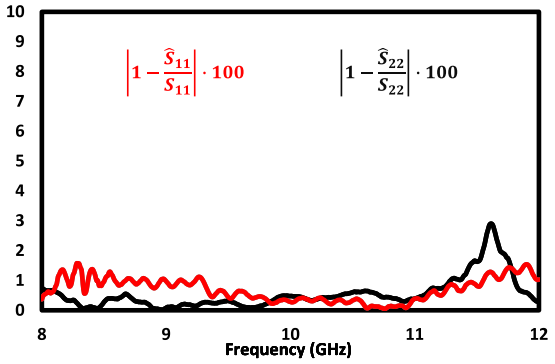

Fig. 3. Percentage errors between measured (S_{11} and S_{22}) and calculated by (1c) ($\hat{S}_{11}$ and $\hat{S}_{22}$) reflections of the waveguide Magic T shown in Fig. 1, with one port of a collinear arm short circuited.

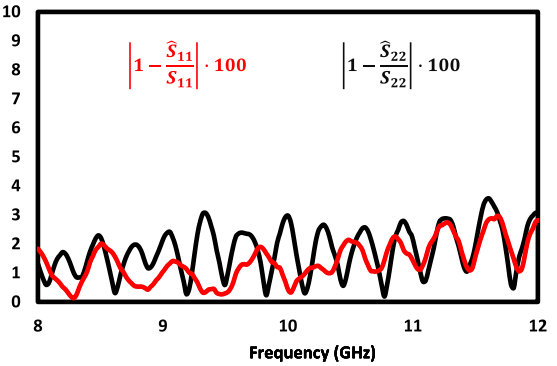

Fig. 4. Percentage errors between measured (S_{11} and S_{22}) and calculated by (1c) ($\hat{S}_{11}$ and $\hat{S}_{22}$) reflections of the E-plane T-junction of [10].

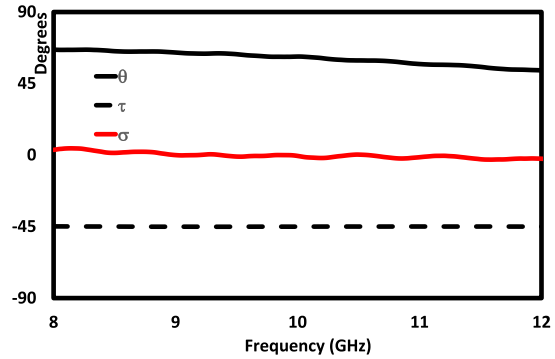

Fig. 5. Parameters ϑ, τ, σ (degrees) for the E-plane T-junction considered in [10].

In fact, with the above triplet, only $\hat{S}_{33}$ is exactly equal to S_{33} but the other terms are not. In particular, the relative error of the approximation is in the order of 1% for $\hat{S}_{31}$, $\hat{S}_{32}$ and $\hat{S}_{12}$, since τ and σ directly derives from S_{31}, S_{32}, and S_{12}. The maximum percentage relative deviation of $\hat{S}_{11}$ and $\hat{S}_{22}$ from S_{11} and S_{22}, shown in Fig. 3, is in the order of 3%. This is caused by the error propagation affecting quantities that are combination of approximated terms. In addition, measurements, done by a two-port VNA, are also affected by errors due to the movements of the cables and to the necessary connections/disconnections.

The agreement is satisfactory even in the second experimental example (Fig. 4), concerning a standard E-plane T-junction [15], that, although being nominally symmetrical, actually is not, since one "symmetrical" arm is 0.2 mm longer than the other.

The relevant parameters ϑ, τ, σ, obtained by (7), are shown in Fig. 5. It can be observed that, as predicted by (2b), $\tau \cong -45°$ in the whole band (the slight deviation from $-45°$ depends on the imperfect symmetry), $|\sigma| < 4.3°$ and $50° < \vartheta < 67°$.

V. Conclusion

This article provides the explicit expression of the scattering matrix of a realizable reciprocal and lossless three-port junction, in terms of three bounded real parameters.

Two significant waveguide cases, the first strongly and the second weakly asymmetrical, are examined to demonstrate, also experimentally, the reliability of formulas (1a)–(1c).

Appendix
Proof of the Theorem

Losslessness implies the following relationships to be satisfied:

$$|S_{11}|^2 + |S_{12}|^2 + |S_{13}|^2 = 1 \tag{8a}$$
$$|S_{12}|^2 + |S_{22}|^2 + |S_{23}|^2 = 1 \tag{8b}$$
$$|S_{13}|^2 + |S_{23}|^2 + |S_{33}|^2 = 1 \tag{8c}$$
$$S_{11}S_{12}^* + S_{12}S_{22}^* + S_{13}S_{23}^* = 0 \tag{8d}$$
$$S_{11}S_{13}^* + S_{12}S_{23}^* + S_{13}S_{33}^* = 0 \tag{8e}$$
$$S_{12}S_{13}^* + S_{22}S_{23}^* + S_{23}S_{33}^* = 0. \tag{8f}$$

From (8c), under the hypothesis that S_{13}, S_{23}, and S_{33} are all real, we can set $S_{33} = \cos\vartheta$, $S_{13} = \sin\vartheta\cos\tau$, and $S_{23} = \sin\vartheta\sin\tau$, where ϑ and τ are suitable angles.

With the above positions, from (8e) and (8f), it immediately follows the expression (1c) of S_{11} and S_{22} in terms of S_{12}, ϑ and τ. By substituting in (8d), the expressions of S_{11}, S_{22}, S_{13}, and S_{33} just given, and setting $S_{12} = |S_{12}|e^{j\sigma}$, we find the equation for $|S_{12}|$

$$\frac{|S_{12}|^2}{\cos\tau\sin\tau} + 2\cos\vartheta\cos\sigma|S_{12}| - \sin^2\vartheta\cos\tau\sin\tau = 0. \tag{9}$$

Whose solution is

$$|S_{12}| = -\cos\tau\sin\tau\cos\sigma\cos\vartheta\left(1 \mp \sqrt{1+\frac{\tan^2\vartheta}{\cos^2\sigma}}\right) \geq 0. \tag{10}$$

Since $\tan^2\vartheta/\cos^2\sigma \geq 0$, the sign of the square root in (10) is perfectly determined, namely

1) $\cos\tau\sin\tau\cos\sigma\cos\vartheta \geq 0$

$$|S_{12}| = -\cos\tau\sin\tau\cos\sigma\cos\vartheta\left(1 - \sqrt{1+\frac{\tan^2\vartheta}{\cos^2\sigma}}\right) \tag{11a}$$

2) $\cos\tau\sin\tau\cos\sigma\cos\vartheta < 0$

$$|S_{12}| = -\cos\tau\sin\tau\cos\sigma\cos\vartheta\left(1 + \sqrt{1+\frac{\tan^2\vartheta}{\cos^2\sigma}}\right). \tag{11b}$$

This proves the theorem.

REFERENCES

[1] *Basic Network Theory*. Accessed: Dec. 1, 2023. [Online]. Available: https://www.microwaves101.com/

[2] C. G. Montgomery, R. H. Dicke, and E. M. Purcell, "Principles of microwave circuits," in *Waveguide Junction with Several Arms*. New York, NY, USA: McGraw-Hill, 1948.

[3] N. Marcuvitz, *Waveguide Handbook*. New York, NY, USA: McGraw-Hill, 1951.

[4] R. E. Collin, *Foundations for Microwave Engineering*, 2nd ed., New York, NY, USA: McGraw-Hill, 1992.

[5] O. R. Price and J. Leichter, "Scattering matrix for an N-port power-divider junction," *IRE Trans. Microw. Theory Tech.*, vol. 8, no. 6, p. 669, 1960.

[6] H. F. Mathis, "Design of lossless junction, given one row in its scattering matrix," *IEEE Trans. Microw. Theory Techn.*, vol. MTT-14, no. 3, p. 159, Mar. 1966.

[7] H. Butterweck, "Scattering bounds for the general lossless reciprocal three-port," *IEEE Trans. Circuit Theory*, vol. CT-13, no. 3, pp. 290–293, Sep. 1966.

[8] A. Morini and T. Rozzi, "Constraints to the optimum performance and bandwidth limitations of diplexers employing symmetric three-port junctions," *IEEE Trans. Microw. Theory Techn.*, vol. 44, no. 2, pp. 242–248, Feb. 1996.

[9] J. Joubert and S. R. Rengarajan, "Design of unequal H-plane waveguide-power dividers for array applications," in *Proc. IEEE Antennas Propag. Soc. Int. Symp. Dig.*, vol. 3, Baltimore, MD, USA, Sep. 1996, pp. 1636–1639.

[10] K. Erkelenz, N. Sielck, A. Sieganschin, T. Jaschke, and A. F. Jacob, "A compact SIW K-/Ka-band diplexer with integrated reactive power divider," in *IEEE MTT-S Int. Microw. Symp. Dig.*, Atlanta, GA, USA, Jun. 2021, pp. 489–491.

[11] J. L. Cano, A. Mediavilla, S. Dragas, and A. Tazon, "Novel square-waveguide dual-mode two-way reactive power divider," *IEEE Trans. Microw. Theory Techn.*, vol. 68, no. 3, pp. 980–986, Mar. 2020.

[12] C. J. R. Smith and H. H. Sigmarsson, "Microstrip T-junction power divider with exponentially tapered transmission lines," *IEEE Microw. Wireless Compon. Lett.*, vol. 26, no. 12, pp. 987–989, Dec. 2016.

[13] J. Esteban and C. Camacho-Peñalosa, "Compact orthomode transducer polarizer based on a tilted-waveguide T-junction," *IEEE Trans. Microw. Theory Techn.*, vol. 63, no. 10, pp. 3208–3217, Oct. 2015.

[14] J. Helszajn, M. Caplin, J. Frenna, and B. Tsounis, "Characteristic planes and scattering matrices of e and H-plane waveguide tee junctions," *IEEE Microw. Wireless Compon. Lett.*, vol. 24, no. 4, pp. 209–211, Apr. 2014.

[15] A. Morini, T. Rozzi, M. Farina, and P. Angeletti, "Scattering matrix of a reciprocal, lossless, and symmetrical three-port power divider," *IEEE Microw. Wireless Technol. Lett.*, vol. 33, no. 2, pp. 130–132, Feb. 2023.

[16] K. Madsen, "An algorithm for minimax solution of overdetermined systems of non-linear equations," *IMA J. Appl. Math.*, vol. 16, no. 3, pp. 321–328, 1975.

[17] A. Morini and L. Zappelli, "Estimation of the losses of 1:N dividers by the measurement of the reflection when the outputs are shorted," *IEEE Trans. Microw. Theory Techn.*, vol. 68, no. 8, pp. 3592–3601, Aug. 2020.

Open Access funding provided by 'Università Politecnica delle Marche' within the CRUI CARE Agreement